Structural basis for HLA-DQ2-mediated presentation of gluten epitopes in celiac disease

Chu-Young Kim[†‡§], Hanne Quarsten[§¶], Elin Bergseng[¶], Chaitan Khosla[†‡‖††], and Ludvig M. Sollid[¶†††]

Departments of [†]Chemical Engineering, [‡]Chemistry, and [‖]Biochemistry, Stanford University, Stanford, CA 94305; and [¶]Institute of Immunology, University of Oslo, and Rikshospitalet University Hospital, N-0027 Oslo, Norway

Edited by Jack L. Strominger, Harvard University, Cambridge, MA, and approved December 31, 2003 (received for review October 27, 2003)

Celiac disease, also known as celiac sprue, is a gluten-induced autoimmune-like disorder of the small intestine, which is strongly associated with HLA-DQ2. The structure of DQ2 complexed with an immunogenic epitope from gluten, QLQPFPQPELPY, has been determined to 2.2-Å resolution by x-ray crystallography. The glutamate at P6, which is formed by tissue transglutaminase-catalyzed deamidation, is an important anchor residue as it participates in an extensive hydrogen-bonding network involving Lys-β71 of DQ2. The gluten peptide–DQ2 complex retains critical hydrogen bonds between the MHC and the peptide backbone despite the presence of many proline residues in the peptide that are unable to participate in amide-mediated hydrogen bonds. Positioning of proline residues such that they do not interfere with backbone hydrogen bonding results in a reduction in the number of registers available for gluten peptides to bind to MHC class II molecules and presumably impairs the likelihood of establishing favorable side-chain interactions. The HLA association in celiac disease can be explained by a superior ability of DQ2 to bind the biased repertoire of proline-rich gluten peptides that have survived gastrointestinal digestion and that have been deamidated by tissue transglutaminase. Finally, surface-exposed proline residues in the proteolytically resistant ligand were replaced with functionalized analogs, thereby providing a starting point for the design of orally active agents for blocking gluten-induced toxicity.

Celiac disease, also known as celiac sprue, is a prevalent disorder (1:200 in many populations) with autoimmune features. It affects the small intestine after dietary exposure to wheat gluten (composed of gliadins and glutenins) and similar prolamin proteins of rye (hordeins) and barley (secalins) (1). Activation of gluten-reactive $CD4^+$ T cells within the intestinal mucosa controls disease development. Classic early-childhood symptoms include chronic diarrhea, abdominal distension, and failure to thrive (2), whereas patients diagnosed later in life display anemia, fatigue, weight loss, diarrhea, and neurological symptoms (3). The only effective treatment available for celiac disease patients today is a strict exclusion of gluten from their diet. Noncompliance to gluten-free diet is associated with increased risk of anemia, infertility, osteoporosis, and intestinal lymphoma (3). Celiac disease is a polygenic disorder, and HLA is the single most important genetic factor (4). The primary HLA association in the great majority of celiac disease patients is with DQ2 (DQA*05/DQB1*02) and in a minority of patients with DQ8 (DQA1*03/DQB1*0302) (5). Gluten-reactive T cells recognize peptides from gluten in the context of HLA-DQ2 or HLA-DQ8, but not in the context of any other HLA molecules expressed by patients (6, 7). Of the many HLA-associated disorders, celiac disease has one of the better-understood pathogenesis.

Although numerous gluten epitopes have been identified to date, some of them appear to be more important, as they are recognized by intestinal T cells from most adult celiac disease patients, whereas others are recognized by only a minority of patients (4). Three DQ2-restricted gliadin epitopes are shown in Table 1. A common feature among these epitopes is the presence of multiple Pro and Gln residues, which gives rise to three unique structural and functional properties. First, these peptides are exceptionally resistant to proteolysis by gastric, pancreatic, and intestinal digestive proteases because of their high Pro content (10). As a result, a high intestinal concentration of potentially immunoreactive peptides is maintained following a gluten-containing diet. Second, the Pro-rich gliadin peptides naturally adopt a left-handed polyproline II (PPII) helical conformation, which is the preferred conformation of all bound MHC class II ligands. For example, the PPII helical structure of unbound PQPQLPY, a motif found in immunodominant α-gliadin epitopes, has recently been confirmed by circular dichroism and NMR spectroscopic analysis (11). Third, selected glutamine residues in these Pro- and Gln-rich gluten peptides are deamidated by tissue transglutaminase (TG2) under physiological conditions, leading to enhanced immunogenicity (Table 1) (4). For example, the α-gliadin peptide PFPQPQLPY, which is almost nonstimulatory to T cells, is selectively deamidated by TG2 to yield PFPQPELPY, a potent antigen (8). Notably, TG2 has specificity toward Pro-rich peptides (12, 13), and there is a good correlation between PPII propensity of gluten peptides and its specificity as a substrate for TG2 (11). Therefore, the helical nature of αI-gliadin appears to facilitate the "activation" of these peptides by rendering it a better substrate for TG2.

Here, we report the x-ray crystal structure of the soluble domain of HLA-DQ2 bound to the deamidated gluten epitope αI-gliadin, PFPQPELPY, and address the following key questions. How does the Pro-rich sequence of αI-gliadin affect MHC binding? What is the structural basis for increased immunogenicity of deamidated gluten peptides? Why is HLA-DQ2 uniquely suited for presentation of gluten-derived epitopes? Our results present an opportunity to decode the immunopathogenic basis of celiac disease and raise the prospect of pharmacological intervention of celiac disease at the MHC level.

Materials and Methods

Expression, Purification, and Crystallization. The soluble extracellular domains of the DQ2 α- and β-chains were coexpressed in insect cells by using a baculovirus expression system and affinity-purified by using the anti-DQ2 mAb 2.12.E11 (14). The sequence QLQPFPQPELPY was fused to the N-terminal end of DQ2 β-chain by a 15-residue linker (15). A complementary Fos/Jun leucine zipper pair was engineered at the C-terminal ends of α- and β-chains, respectively, with intervening factor Xa proteolysis sites, to increase the heterodimer stability during protein expression, analogous to earlier works by Teyton and coworkers (16) and Wucherpfennig and coworkers (17). Leucine zippers were removed from DQ2 by factor Xa digestion before crystal-

IMMUNOLOGY

This paper was submitted directly (Track II) to the PNAS office.

Abbreviations: PPII, polyproline II; TG2, transglutaminase.

Data deposition: The atomic coordinates for the HLA-DQ2–αI-gliadin complex have been deposited in the Protein Data Bank, www.pdb.org (PDB ID code 1S9V).

[§]C.-Y.K. and H.Q. contributed equally to this work.

[††]To whom correspondence may be addressed. E-mail: ck@chemeng.stanford.edu or l.m.sollid@labmed.uio.no.

Table 1. HLA-DQ2-restricted gliadin epitopes

Epitope	Recognized by celiac disease patients	Amino acid sequence									
		P-1	P1	P2	P3	P4	P5	P6	P7	P8	P9	P10
αI-gliadin (8)	Frequently	Q	P	F	P	Q	P	E	L	P	Y	—
αII-gliadin (8)	Frequently	—	P	Q	P	E	L	P	Y	P	Q	P
γI-gliadin (9)	Infrequently	Q	P	Q	Q	S	F	P	E	Q	E	R

Glutamate (E) that is converted from glutamine (Q) by tissue transglutaminase-catalyzed deamidation is underlined.

lization. Factor Xa-processed DQ2 was further purified by anion-exchange chromatography and size-exclusion chromatography, then concentrated to 4 mg/ml in 25 mM Tris·HCl, pH 8.0. Crystals of the DQ2–αI complex were obtained by using the hanging drop method. Typically, 2 μl of protein solution (2–4 mg/ml DQ2/25 mM Tris·HCl, pH 8.0) and 2 μl of precipitant buffer (50 mM sodium acetate, pH 3.5/200 mM ammonium acetate/40 mM ammonium sulfate/4% ethylene glycol/26% PEG 3350) were combined in a single drop hanging over 1 ml of precipitant buffer at room temperature. Small crystals appeared within 3 days and grew to full size in 2 weeks. Crystals were soaked in a cryoprotectant buffer containing 28% ethylene glycol, 50 mM sodium acetate (pH 3.5), 200 mM ammonium acetate, 40 mM ammonium sulfate, and 26% PEG 3350 for 2 h and then frozen in liquid nitrogen.

Structure Determination. The structure of DQ2–αI-gliadin complex was determined to 2.2-Å resolution by x-ray crystallography. Crystal belonged to the $P2_12_12_1$ space group with cell dimensions $a = 91.11$ Å, $b = 93.75$ Å, and $c = 102.72$ Å. Statistics for data collection and structure refinement are summarized in Table 2. X-ray diffraction data were collected from a single crystal at beamline 11-1 of the Stanford Synchrotron Radiation Laboratory by using a Quantum 315 charge-coupled device detector. Oscillation images were processed with DENZO, and data reduction was carried out with SCALEPACK (18). The structure of the DQ2–αI complex was determined by molecular replacement using the program AMORE (19) in the CCP4 suite of programs (20). The 2.4-Å resolution structure of insulin peptide–HLA-DQ8 complex (PDB ID code 1JK8) (21) minus the insulin peptide and solvent molecules was used as the search model. After initial refinement with the maximum-likelihood function of program REFMAC (22), iterative cycles of refinement including simulated annealing, temperature factor refinement, and energy minimization were made with the program CNS (23). Model building and correction were performed by using σ_A-weighted $F_o - F_c$ and $2F_o - F_c$ electron density maps with the program O (24). There are two molecules of DQ2 in the asymmetric unit, which are arranged in an offset, parallel manner (referred to as DQ2-I and DQ2-II). Superposition of the α- and β-chains of DQ2-I onto that of DQ2-II gives an rms deviation of 0.4 Å (Cα only). There are two notable differences in the bound gliadin peptide of each DQ2 heterodimer. First, the side chain of the P9 Tyr residue is only visible in DQ2-II (chain ID: D, E, F). Second, the orientation of P2 Phe side chain is slightly different in the two complexes, although in both cases it points away from the DQ2 ligand-binding site. In DQ2-I (chain ID: A, B, C), residues α1a-1b, α1, α181–191, β1–2, β106–112, β135 side chain, and β191–198 are absent from the final model because of the lack of electron density in the corresponding region. For DQ2-II, electron density is absent for residues α1a-1b, α1, α180–191, β1–2, β105–112, β135 side chain, β136-side chain, and β191–198. All figures, distances, and area measurements in this article are derived from DQ2-II. Numbering of the HLA-DQ2 residues is based on sequence homology with HLA-DR1 and is given in Fig. 4, which is published as supporting information on the PNAS web site. Atomic coordinates of the αI-gliadin–HLA-DQ2 complex have been deposited in the Protein Data Bank (PDB ID code 1S9V).

Results and Discussion

Overall Structure. The DQ2 structure exhibits the classic MHC class II folding motif. The N-terminal domains of the DQ2 heterodimer combine to form the peptide-presenting groove: a five-turn α-helix (from DQ2 α-chain) runs parallel to a longer, but kinked α-helix (from DQ2 β-chain), forming the side walls of the peptide-binding groove. The two helices sit on top of an eight-stranded β-sheet platform, contributed equally from the DQ2 α- and β-chains. Eleven αI-gliadin residues (LQPFPQPELPY) are clearly visible in the experimental electron density map, occupying the P-2 to P9 register in the peptide-binding groove of DQ2 (Fig. 1*A*). The side-chain atoms of P-1 and P-2 are presumably disordered and are absent in the final model. αI-gliadin residues Gln, Glu, and Leu occupy the P4, P6, and P7 pockets of DQ2, respectively (Fig. 1*B*). This register is in keeping with previous binding data (8). Overall, DQ2 and

Table 2. Data collection and refinement statistics

Data collection	
Resolution range, Å	40.0 to 2.2
Unique reflections	44,458 (1,677)
Total no. of reflections	288,797 (4,689)
Completeness, %	93.9 (76.5)
$I/\sigma(I)$	7.8 (2.182)
R_{merge},* %	9.2 (35.1)
Refinement statistics	
Resolution range, Å	40.0 to 2.2
Number of reflections	38,843
R_{work}†	0.221 (0.294)
R_{free}‡	0.283 (0.348)
Estimated coordinate error (Å)	0.3
rms deviations	
Bonds	0.006
Angles	1.4
Dihedrals	26.2
Impropers	0.8
Ramachandran plot	
Favored, %	91.2
Allowed, %	7.9
Generous, %	0.5
Disallowed, %	0.5

Numbers in parentheses refer to statistics for the highest 2.26- to 2.22-Å resolution shell.

*R_{merge} for replicate reflections, $R_{merge} = \Sigma|I_h - \langle I_h\rangle|/\Sigma\langle I_h\rangle$; I_h = intensity measured for reflection h; $\langle I_h\rangle$ = average intensity for reflection h calculated from replicate data.

†Crystallographic R factor, $R_{cryst} = \Sigma\|F_o| - |F_c\|/\Sigma|F_o|$; $|F_o|$ and $|F_c|$ are the observed and calculated structure factor amplitudes, respectively, for those reflections not included in the R_{free} test set.

‡Free R factor, $R_{free} = \Sigma\|F_o| - |F_c\|/\Sigma|F_o|$ for only those reflections included in the R_{free} test set.

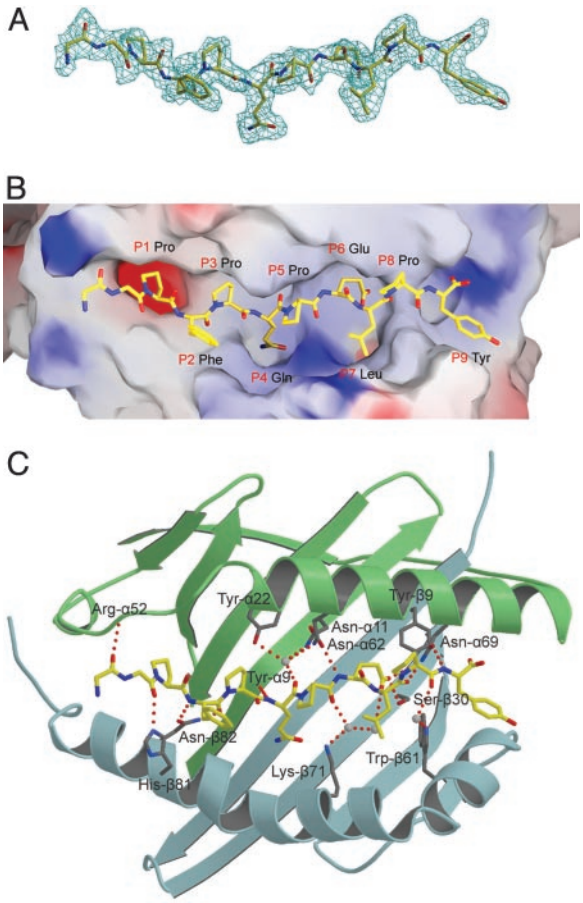

Fig. 1. (*A*) Difference electron density map calculated with Fourier coefficients $|F_o| - |F_c|$ and phases derived from the final model less the αI-gliadin peptide and solvent molecules. Map is contoured at 2.8 σ. There are extra amino acids on either side of the P2–P9 residues of the peptide–DQ2 construct that are not modeled because of a lack of electron density. (*B*) GRASP (25) generated the electrostatic potential surface of HLA-DQ2 (red region, negative; blue region, positive) with the bound αI-gliadin peptide (C, white; N, blue; O, red). (*C*) Putative hydrogen-bonding network in the DQ2–αI-gliadin complex (shown as red dashes). αI-gliadin is shown in yellow (C, yellow; N, blue; O, red). Backbone structure of HLA-DQ α- and β-chains are shown in green and blue ribbon plots, respectively, and side chains engaged in hydrogen bonding are shown in gray (C, gray; N, blue; O, red). Gray spheres represent water molecules.

αI-gliadin share 1,032 Å^2 of contact surface area, which is comparable to 1,083 Å^2, 930 Å^2, and 904 Å^2 of DQ8–, DR1–, and DR3–ligand complexes (21, 26, 27), respectively. There are 13 hydrogen bonds between the main-chain atoms of αI-gliadin and HLA-DQ2 (Fig. 1*C*). Ten interactions are mediated by conserved MHC residues (Arg-α52—CO^{P-2}, His-β81—CO^{P-1}, Asn-β82—NH^{P2}, Asn-β82—CO^{P2}, Asn-α62—H_2O—CO^{P4}, Asn-α11—H_2O—CO^{P4}, Asn-α62—NH^{P6}, Asn-α69—CO^{P7}, Trp-β61—H_2O—CO^{P8}, Asn-α69—NH^{P9}), whereas three interactions are mediated by polymorphic MHC residues (Tyr-α9—NH^{P4}, Tyr-α22—H_2O—CO^{P4}, Lys-β71—H_2O—CO^{P5}). Of the structurally characterized HLA molecules, DQ2 has the strongest similarity to DQ8 (rms deviation: 1.5 Å; Cα only). As is the case in DQ8, there is no salt bridge between residues Asp-β57 and Arg-α76. There is one noticeable difference in the backbone structure of DQ2 and DQ8. In comparison with the DQ8 structure, the short α-helix (corresponding to residues α45–α51) in DQ2 is shifted towards the long α-helical stretch of the α-chain, presumably influenced by the deletion mutation at

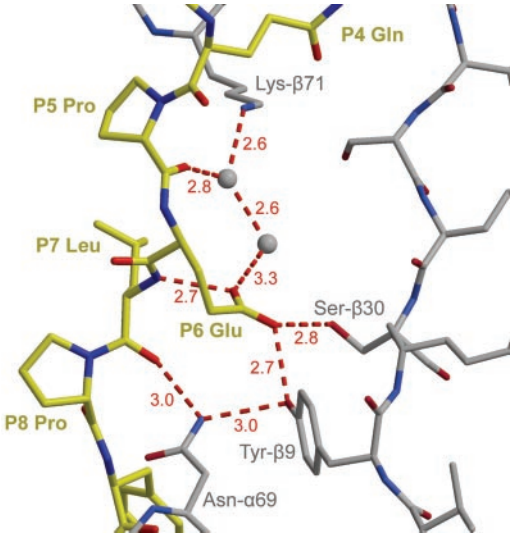

Fig. 2. Hydrogen-bonding network in the epitope-binding site of DQ2. αI-gliadin is shown in yellow (C, yellow; N, blue; O, red), and HLA-DQ2 α- and β-chains are shown in gray (C, gray; N, blue; O, red). Gray spheres represent water molecules. Atom-to-atom distances are given in Å.

α53. The binding site topology and charge distribution of DQ2 and DQ8 are dissimilar. Particularly striking is a unique positive electrostatic region between the P4 and P6/P7 pockets in DQ2 caused by Lys-β71 (Fig. 1*B*). DQ8 contains a Thr at β71 and has an overall neutral electrostatic potential in this region. Consistent with the structural differences, there are no data available indicating that the αI-gliadin epitope is recognized in the context of DQ8 in celiac disease patients.

Peptide Interaction at P6. The P6 Glu of αI-gliadin, which is formed by TG2-catalyzed deamidation, participates in an extensive hydrogen-bonding network (Fig. 2). Although the DQ2-specific residue, Lys-β71, plays a key role in stabilizing this residue, the x-ray structure reveals a surprisingly complex network of noncovalent interactions. One carboxylate oxygen atom accepts hydrogen bonds from the side chains of Ser-β30 and Tyr-β9, whereas the second oxygen atom accepts hydrogen bonds from the backbone nitrogen of αI-gliadin itself and also from a water molecule. This water molecule is hydrogen-bonded to a second water molecule, which in turn hydrogen-bonds to an αI-gliadin backbone oxygen atom and the side-chain NH group of Lys-β71. If Gln were present at this position instead of Glu (i.e., the nondeamidated native gliadin peptide), this intricate hydrogen-bonding network would be disrupted, because the amide nitrogen is not a good hydrogen-bond acceptor. Also, the Gln carbonyl oxygen is a less attractive hydrogen-bond acceptor than the negatively charged Glu carboxylate oxygen. Coupling energies of up to 4 kcal/mol have been measured for hydrogen bonds involving charged–neutral partners (28). *In vitro* binding assay shows that the deamidated αI-gliadin has a 25-fold higher affinity compared with the nondeamidated counterpart (IC_{50} of 100 vs. 4 μM) (8), which may be partially due to having a more potent hydrogen-bond acceptor that can form additional protein-to-protein hydrogen bonds, resulting in a more stable gliadin–DQ2 complex.

Peptide Interaction at P9. Bulky hydrophobic residues at the P9 position have been identified as optimal anchor residues for other DQ2 ligands (29). Surprisingly, the C-terminal Tyr side chain of αI-gliadin is positioned outside the P9 pocket (Fig. 1*B*). This may reflect more binding energy gained from contacting the

α-helical wall of the β-chain side of the peptide-binding groove. Alternatively, the rigid Pro at P8, which lies over a prominent ridge in the binding site formed by Asn-α69, Val-β38, and Trp-β61, perturbs the docking of Tyr into the P9 pocket, making this residue less important for binding of αI-gliadin to DQ2.

Peptide Interactions at P1, P4, and P7. Binding studies have indicated that HLA-DQ2 anchor peptides by side-chain interactions at the P1, P4, and P7 residues in addition to those at P6 and P9 (30–33). In the αI-gliadin–HLA-DQ2 structure, the Pro at P1, Gln at P4, and Leu at P7 make van der Waals interaction with the pocket wall. These residues, however, are not optimal anchors at these positions for DQ2 (30–33). The nonoptimal interactions at these pockets may explain why the αI epitope is not among the best DQ2 ligands described (8). To note, however, in other DQ2-restricted gliadin epitopes (Table 1), interactions of negatively charged glutamic acid at P4 or P7 seem to be important (see below).

HLA-DQ2 and Presentation of Gliadin Epitopes. The αI-gliadin—HLA-DQ2 structure described here allows us to address the question of why DQ2 is especially well suited to binding and presenting gliadin epitopes. It has been suggested that Arg-β70 and Lys-β71 are responsible for the preference for binding negatively charged residues at the P4, P6, and P7 pockets (30–33), analogous to what has been described for rheumatoid arthritis and HLA-DR4 (34–36). The Arg-β70 side chain points toward the solvent, where the guanidinium side chain is held by a hydrogen bond to the main-chain CO group of Asp-β66 but is still well situated to confer a negative charge preference at the P7 pocket. In addition, Lys-β71 is positioned to interact favorably with a negatively charged residue in the P4, P6, or P7 register. Because TG2-catalyzed deamidation typically generates gluten epitopes with a negatively charged Glu residue in one of these registers (Table 1), the charge complementation afforded by Arg-β70 and Lys-β71 may be essential and critical in the pathogenesis of celiac disease.

The multiple Pro residues in gluten-derived epitopes gives rise to a second selectivity filter for MHC binding that is independent of side-chain interactions (Fig. 3). Most of the energy for binding of peptides to MHC class II results from a network of hydrogen bonds to the peptide main chain (26). Typically, hydrogen bonds between conserved MHC residues and amide nitrogen atoms of the P1, P2, P4, P6, and P9 residues participate in this network. The presence of a Pro residue in any of these positions eliminates this possibility. This results in a substantial reduction in the number of registers available for gluten peptides to bind to MHC class II. The αI-gliadin, which contains four Pro residues, binds to HLA-DQ2 in a register that still retains critical hydrogen bonds between the MHC and the peptide backbone (Fig. 1*C*). One implication of such register constraint is that the number of MHC class II molecules that can bind a Pro-rich peptide in the required register yet also establish favorable interactions with the peptide side chains is greatly reduced. This is likely the major factor to explain why DQ2 with its ability to accommodate negatively charged residues at P4, P6, or P7 is superior to bind and present Pro-rich gluten peptides.

In most MHC class II molecules, a hydrogen bond is observed between the amide nitrogen of the P1 residue and the backbone carbonyl of residue α53 (26, 27, 37, 38). Some DQA1 alleles, including DQA1*0501, have a single residue deletion at this position, which may prevent this noncovalent interaction. If DQ2 is unable to form a hydrogen bond to the backbone NH group at P1, then presumably Pro could be accommodated at this location without significant penalty. This idea is consistent with the observation that Pro residues are often found at P1 of gluten-derived DQ2 epitopes.

In addition to Lys-β71, at least one more polymorphic DQ2 residue hydrogen-bonds with a backbone NH in αI-gliadin. Through a network of water-mediated hydrogen bonds, the phenolic OH of Tyr-α22 bonds to the P4 carbonyl oxygen (Fig. 1*C*) and presumably contributes to selective presentation of αI-gliadin. Interestingly, the closely related HLA DQA1*0201/DQB1*0202, which has only 10 different residues in the ligand-binding domains from DQA1*0501/DQB1*0201, has a Phe residue at the corresponding position and is not associated with celiac disease (5).

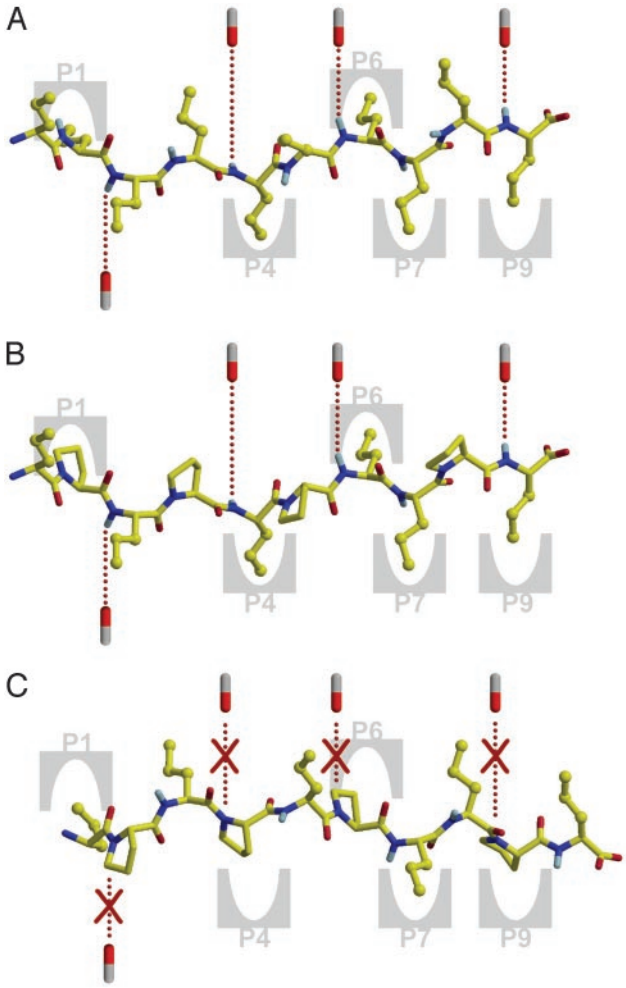

Fig. 3. (*A*) Binding of a peptide that does not contain any Pro residues to HLA-DQ2. A number of peptide main-chain NH groups form hydrogen bonds in the peptide binding site. Several peptide side-chains dock into binding pockets (P1, P4, P6, P7, P9) of the HLA molecule, providing additional binding energy and serving as a selectivity filter. (*B*) Binding of a Pro-rich peptide (such as the αI-gliadin) to HLA-DQ2 in a favorable register. Hydrogen-bond interactions involving peptide main-chain NH groups are still established, although there is significantly less main-chain NH groups available. (*C*) The same peptide in a shifted register cannot form such hydrogen bonds. Similarly, peptides that have Pro at unfavorable locations cannot form such hydrogen bonds, thereby limiting the registers available for binding.

Proline-Induced Ligand Rigidity. The αI-gliadin–HLA-DQ2 structure moreover suggests an unusual principle for MHC class II–ligand interactions. HLA receptors induce a PPII conformation in their ligands, which presumably exist as random coils in solution. The Pro-rich character of gluten epitopes enhances their propensity to naturally adopt a PPII conformation (11). We hypothesize that the binding of gluten peptides to HLA is partially dictated by a lock-and-key principle. The magnitude of

such an entropic advantage is difficult to determine experimentally. In one example, a 420-fold increase in binding affinity is observed in the inhibition of penicillopepsin by a macrocyclic pentapeptide inhibitor vs. its acyclic analog, despite the fact that respective x-ray crystal structure shows nearly identical inhibitor conformation and interaction (39).

In summary, the PPII character of αI-gliadin, the maintenance of the backbone hydrogen-bonding network despite the many Pro residues, and the interaction of a TG2-generated negative charge with the P6 pocket, make this epitope a good ligand for HLA-DQ2. The HLA association in celiac disease can be explained by a superior ability of DQ2 to bind the biased repertoire of Pro-rich gluten peptides that have survived gastrointestinal digestion and that have been deamidated by TG2. Our co-crystal structure may now be exploited for designing a therapeutically effective DQ2 blocking agent that precludes the stimulation of celiac disease-specific T cells by gluten-derived epitopes (4, 40, 41). Although such inhibitors of MHC class II-mediated antigen presentation to disease-specific T cells have shown promise in the context of other autoimmune disorders (42), therapeutic intervention by this mechanism has proven challenging because of low systemic bioavailability and high proteolytic susceptibility of a therapeutic peptide. Fortunately, inflammation in celiac disease is localized to the gut, and as such the bioavailability of DQ2 inhibitors is unlikely to be a major stumbling block. Moreover, the αI-gliadin epitope has been shown to be resistant to gastrointestinal proteolysis (8); therefore, an analog with the same Pro-rich scaffold is expected to have good pharmacokinetic properties. We synthesized αI-gliadin analogs where P5 Pro and P8 Pro were substituted with γ-hydroxyproline. These positions were selected because Pro side chains at P5 and P8 are mostly solvated and make limited interaction with DQ2. Binding assays (as in ref. 30) show that these analogs bind to DQ2 with similar affinity as αI-gliadin. Additional chemical groups can therefore be attached to the engineered hydroxyl moiety at P5 and/or P8, thereby altering the αI-gliadin–DQ2 surface landscape, and potentially inhibiting gluten presentation to disease-specific T cells.

This paper is dedicated to the memory of Don C. Wiley. We thank Dr. Michael Rynkiewicz for helpful discussions on x-ray crystallography. Portions of this research were carried out at the Stanford Synchrotron Radiation Laboratory, a national user facility operated by Stanford University on behalf of the U.S. Department of Energy Office of Basic Energy Sciences. Research in our laboratories was supported by National Institutes of Health Grant DK65965 (to C.K.) and grants from the Research Council of Norway and the Norwegian Cancer Society (to L.M.S.). H.Q. is a postdoctoral fellow of the Norwegian Cancer Society.

1. Trier, J. S. (1991) *N. Engl. J. Med.* **325,** 1709–1719.
2. Schmitz, J. (1992) in *Coeliac Disease*, ed. Marsh, M. N. (Blackwell, Oxford), pp. 17–48.
3. Maki, M. & Collin, P. (1997) *Lancet* **349,** 1755–1759.
4. Sollid, L. M. (2002) *Nat. Rev. Immunol.* **2,** 647–655.
5. Sollid, L. M. & Thorsby, E. (1993) *Gastroenterology* **105,** 910–922.
6. Lundin, K. E., Scott, H., Hansen, T., Paulsen, G., Halstensen, T. S., Fausa, O., Thorsby, E. & Sollid, L. M. (1993) *J. Exp. Med.* **178,** 187–196.
7. Lundin, K. E., Gjertsen, H. A., Scott, H., Sollid, L. M. & Thorsby E. (1994) *Hum. Immunol.* **41,** 24–27.
8. Arentz-Hansen, H., Korner, R., Molberg, O., Quarsten, H., Vader, W., Kooy, Y. M. C., Lundin, K. E. A., Koning, F., Roepstorff, P., Sollid, L. M., *et al*. (2000) *J. Exp. Med.* **191,** 603–612.
9. Sjostrom, H., Lundin, K. E. A., Molberg, O., Korner, R., McAdam, S. N., Anthonsen, D., Quarsten, H., Noren, O., Roepstorff, P., Thorsby, E., *et al*. (1998) *Scand. J. Immunol.* **48,** 111–115.
10. Hausch, F., Shan, L., Santiago, N. A., Gray, G. M. & Khosla, C. (2002) *Am. J. Physiol.* **283,** G996–G1003.
11. Parrot, I., Huang, P. C. & Khosla, C. (2002) *J. Biol. Chem.* **277,** 45572–45578.
12. Vader, L. W., de Ru, A., van der Wal, Y., Kooy, Y. M. C., Benckhuijsen, W., Mearin, M. L., Drijfthout, J. W., van Veelen, P. & Koning, F. (2002) *J. Exp. Med.* **195,** 643–649.
13. Fleckenstein, B., Molberg, O., Qiao, S.-W., Schmid, D. G., von der Mulbe, F., Elgstoen, K., Jung, G. & Sollid, L. M. (2002) *J. Biol. Chem.* **277,** 34109–34116.
14. Quarsten, H., McAdam, S. N., Jensen, T., Arentz-Hansen, H., Molberg, O., Lundin, K. E. A. & Sollid, L. M. (2001) *J. Immunol.* **167,** 4861–4868.
15. Kozono, H., White, J., Clements, J., Marrack, P. & Kappler, J. (1996) *Nature* **369,** 151–154.
16. Scott, C. A., Garcia, K. C., Carbone, F. R., Wilson, I. A. & Teyton, L. (1996) *J. Exp. Med.* **183,** 2087–2095.
17. Kalandadze, A., Galleno, M., Foncerrada, L., Strominger, J. L. & Wucherpfennig, K. W. (1996) *J. Biol. Chem.* **271,** 20156–20162.
18. Otwinowski, Z. & Minor, W. (1997) *Methods Enzymol.* **276,** 307–325.
19. Navaza, J. (1944) *Acta Crystallogr. A* **50,** 157–163.
20. Collaborative Computational Project No. 4 (1994) *Acta Crystallogr. D* **50,** 760–763.
21. Lee, K. H., Wucherpfennig, K. W. & Wiley, D. C. (2001) *Nat. Immunol.* **2,** 501–507.
22. Murshudov, G. N., Vagin, A. A. & Dodson, E. J. (1997) *Acta Crystallogr. D* **53,** 240–255.
23. Brunger, A. T., Adams, P. D., Clore, G. M., DeLano, W. L., Gros, P., Grosse-Kunstleve, R. W., Jiang, J.-S., Kuszewski, J., Nilges, M., Pannu, N. S., *et al*. (1998) *Acta Crystallogr. D* **54,** 905–921.
24. Jones, T. A., Zou, J.-Y., Cowan, S. W. & Kjeldgaard, M. (1991) *Acta Crystallogr. A* **47,** 110–119.
25. Nicholls, A., Sharp, K. & Honig, B. (1991) *Proteins Struct. Funct. Genet.* **11,** 281–296.
26. Stern, L. J., Brown, J. H., Jardetzky, T. S., Gorga, J. C., Urban, R. G., Strominger, J. L. & Wiley, D. C. (1994) *Nature* **368,** 215–221.
27. Ghosh, P., Amaya, M., Mellins, E. & Wiley D. C. (1995) *Nature* **378,** 457–462.
28. Fersht, A. R. & Serrano, L. (1993) *Curr. Opin. Struct. Biol.* **3,** 75–83.
29. Quarsten, H., Paulsen, G., Johansen, B. H., Thorpe, C. J., Holm, A., Buus, S. & Sollid, L. M. (1998) *Int. Immunol.* **10,** 1229–1236.
30. Johansen, B. H., Vartdal, F., Eriksen, J. A., Thorsby, E. & Sollid, L. M. (1996) *Int. Immunol.* **8,** 177–182.
31. van de Wal, Y., Kooy, Y. M. C., Drijfhout, J. W., Amons, R. & Koning, F. (1996) *Immunogenetics* **44,** 246–253.
32. Vartdal, F, Johansen, B. H., Friede, T., Thorpe, C. J., Stefanovic, S., Eriksen, J. E., Sletten, K., Thorsby, E., Rammensee, H.-G. & Sollid, L. M. (1996) *Eur. J. Immunol.* **26,** 2764–2772.
33. van de Wal, Y., Kooy, Y. M., Drijfhout, J. W., Amons, R., Papadopoulos, G. K. & Koning, F. (1997) *Immunogenetics* **46,** 484–492.
34. Hammer, J., Gallazzi, F., Bono, E., Karr, R. W., Guenot, J., Valsasnini, P., Nagy, Z. A. & Sinigaglia, F. (1995) *J. Exp. Med.* **181,** 1847–1855.
35. Woulfe, S. L., Bono, C. P., Zacheis, M. L., Kirschmann, D. A., Baudino, T. A., Swearingen, C., Karr, R. W. & Schwartz, B. D. (1995) *Arthritis Rheum.* **38,** 1744–1753.
36. Wucherpfennig, K. W. & Strominger, J. L. (1995) *J. Exp. Med.* **181,** 1597–1601.
37. Smith, K. J., Pyrdol, J., Gauthier, L., Wiley, D. C. & Wucherpfennig, K. W. (1998) *J. Exp. Med.* **188,** 1511–1520.
38. Dessen, A., Lawrence, C. M., Cupo, S., Zaller, D. M. & Wiley, D. C. (1997) *Immunity* **7,** 473–481.
39. Kahn, A. R., Parrish, J. C., Fraser, M. E., Smith, W. W., Bartlett, P. A. & James, M. N. G. (1998) *Biochemistry* **37,** 16839–16845.
40. Schuppan, D. & Hahn, E. G. (2002) *Science* **297,** 2218–2220.
41. Mearin, M. L. & Koning, F. (2003) *J. Pediatr. Gastroenterol. Nutr.* **36,** 9–11.
42. Falcioni, F., Ito, K., Vidovic, D., Belunis, C., Campbell, R., Berthel, S. J., Bolin, D. R., Gillespie, P. B., Huby, N., Olson, G. L., *et al*. (1999) *Nat. Biotechnol.* **17,** 562–567.